Journal of Hydroscience and Hydraulic Engineering
Vol. 18, No.2 November, 2000, 145-156

3-DIMENSIONAL DIFFUSION CHARACTERISTICS OF A SURFACE FORCED PLUME IN COASTAL SEA

By

Masafumi Mizutori, Takaki Tsubono, Shin'ichi Sakai, Norikazu Nakashiki and Shiro Matsunashi

Central Research Institute of Electric Power Industry,
Abiko-shi, Chiba-ken, Japan

SYNOPSIS

The diffusion behavior of a surface forced plume formed by the discharge of heated water from thermal power plant into the coastal sea is investigated by the field observation and the numerical simulation. The distribution and fluctuation of velocity and temperature are measured in the field, then the characteristics of the 3-dimensional velocity and temperature structures, vertical eddy viscosity and diffusivity are obtained. A 3-dimensional turbulence closure model, k-ε model, is applied in order to simulate the behavior of a surface forced plume observed in the field. Performance of the 3-dimensional model is also discussed by comparison of the computational results with the in-situ data.

INTRODUCTION

In many thermal power plants, heated water used for cooling water is discharged into the coastal sea. The heated water discharged by surface discharge forms a surface forced plume. Therefore, it is important in to estimate accurately the diffusion process of such a surface forced plume in natural environment. The diffusion behavior of the surface forced plume is complicated, and affected by its discharge conditions and ambient conditions. Especially in the case of discharge at high velocity, the diffusion process in the area near the outlet depends mainly on its discharge conditions "flow rate, discharge velocity and shape of outlet" and the topography of coastal sea. On the other hand, the diffusion process in the area far from the outlet depends on ambient currents, turbulence and heat exchange at the sea surface. The diffusion behavior of a surface forced plume has been investigated both experimentally and numerically. However, few studies have been concerned with the above mentioned complicated situation.

The purpose of this study is to investigate the diffusion behavior of a surface forced plume formed in the coastal sea by field observation and 3-dimensional numerical simulation. Firstly, the 3-dimensional structure and turbulent characteristics of velocity and temperature of a surface forced plume are investigated by field observation. Especially, the vertical eddy viscosity / diffusivity in the area near the outlet are evaluated. Secondly, a 3-dimensional numerical model is applied to simulate the behavior of a surface forced plume observed in the filed. The applicability of the model is examined by comparing the computational results with observation data.

FIELD OBSERVATION

1. Field and Discharge Conditions

The field observation was conducted in the open-sea area shown in Fig.1 in November 1993. The ambient current is aperiodic in this area. During the observation period, the current flowed southward continuously. The discharge conditions of the power plant concerned are shown in Table 1.

Table 1 Discharge conditions of the power plant

Width of outlet	9m
Flow rate	47.4m³/s
Discharge velocity	about 2m/s
Temperature Difference between ambient water and discharge water	8.4℃
Salinity	33.0
Discharge direction	45° from the shore line

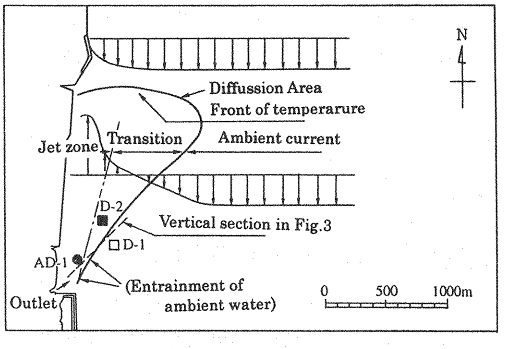

Fig.1 Observation area and schematic horizontal distribution of surface forced plume

2. 3-dimensional structure of surface forced plume

The 3-dimensional distributions of velocity, temperature and salinity in the coastal area were measured using ADCP(Acoustic Doppler Current Profiler) and towed temperature and salinity measuring system.

Fig.2 shows horizontal distributions of velocity vectors and temperature in the layers of 1m and

3m under the sea surface. Though the observed ambient temperatures varied slightly, the mean value was about 15℃. The heated water discharged from the outlet turned immediately to advance along the northward shore line. This behavior seems to indicated the existence of to the larger amount of entrainment from the off-shore side than from the near-shore side. T.
hen, the surface forced plume gradually turned offshore under the influence of southward ambient currents. On the other hand, the velocity distributions along offshore lines indicated that jet zone, transition zone and ambient current zone were formed from near-shore area to off-shore area. Fig.1 shows schematic view of the diffusion pattern of the surface forced plume in this observation.

Fig.3 shows velocity vectors and temperature contours in a vertical section cut along the initial discharge direction at the outlet. The vertical distribution of velocity and temperature were approximately uniform in the area nearer than 300m from the outlet. On the other hand, a warm water layer of 2～3m was formed in the area farther than 400m from the outlet.

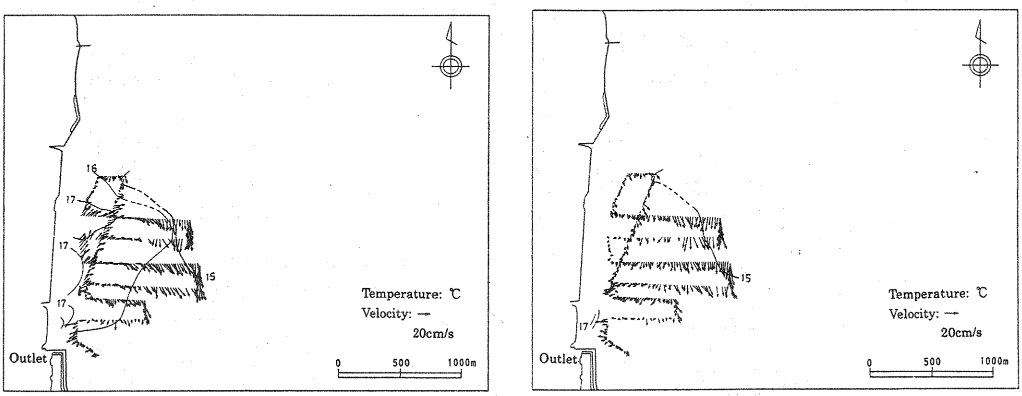

(1) The layer of 1m under the sea surface (2) The layer of 3m under the sea surface
Fig.2 Velocity vectors and temperature contours in horizontal section(Observed Result)

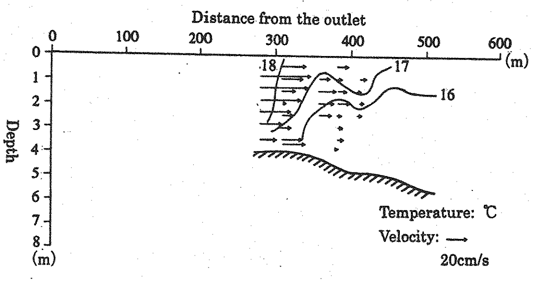

Fig.3 Velocity vectors and temperature contours in vertical section (Observed Result)

3. Turbulence measurements around jet zone

The two methods of field measurement were conducted in order to evaluate the vertical eddy viscosity and diffusivity in the area near the outlet. One was to set up a frame with electromagnetic velocimeter, wave pressure gage and temperature-salinity sensors on the bottom (in Fig.4), and to observe 3-dimensional velocity, hydraulic pressure, temperature and salinity for about 40 hours continuously. When some coefficients were evaluated, the continuous data of 3 hours was selected from data of 40 hours. Velocity and pressure were measured at the point of 3m above the bottom, and temperature and salinity at the point of every 0.5m between 0.5~3.0m above the bottom. The measuring sites are indicated as D-1 and D-2 in Fig.1.

The other was to set up ADCP on the bottom at AD-1 indicated in Fig.1, and to measure 3-dimensional velocity at the point of every 0.5m between 1.25~3.75m above the bottom for 1 hour continuously at intervals of 2 seconds. The vertical distributions of temperature and salinity were measured using CSTD immediately.

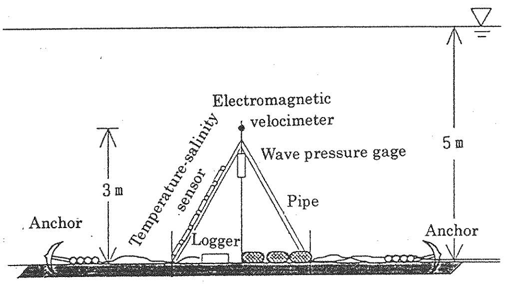

Fig.4 Schematic measuring facility in the field

The following four algorithms were used to calculate the vertical eddy viscosity / diffusivity.

[Vertical eddy viscosity]

1) Algorithm based on auto-correlation coefficient (Az_1)

$$A_{Z_1} = \beta \cdot \overline{w'^2} \int_0^\infty \gamma_w(\tau) d\tau \quad (1)$$

where $\gamma_w(\tau)$: auto-correlation coefficient of vertical velocity, $\beta = 1$.

2) Algorithm based on Reynolds stress (Az_2)

$$A_{Z_2} = \frac{-\overline{u'w'}}{\partial u / \partial z} \quad (2)$$

[Vertical eddy diffusivity]

3) Algorithm based on turbulent heat flux (Kz_1)

$$K_{Z_1} = \frac{-\overline{T'w'}}{\partial T / \partial z} \quad (3)$$

4) Algorithm based on energy dissipation

$$K_{Z_2} = \frac{0.2\varepsilon}{N} \tag{4}$$

where N: Brunt-Vaisala frequency, ε : dissipation rate.

The wave-induced velocity with the period of about 10 seconds is remarkably observed in this observation data. Therefore these components were excluded from original data when the vertical eddy viscosity and diffusivity were calculated. The excluding method based on the linear regression function between vertical velocity and hydraulic pressure, shown in Fig.5, was used to analyze the data at D-1 and D-2. Fig.6 shows energy spectra of vertical velocity fluctuation obtained after excluding excluded the above mentioned periodic components. On the other hand, the method to do moving average for the data of every 20 seconds was used at AD-1, because water pressure was not observed here.

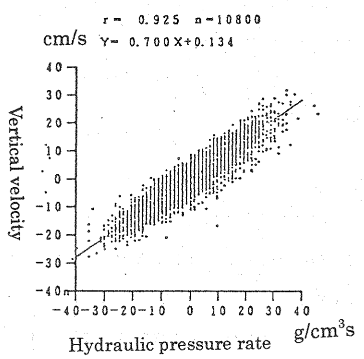

Fig.5 Relation between vertical velocity and hydraulic pressure rate (At D-2)

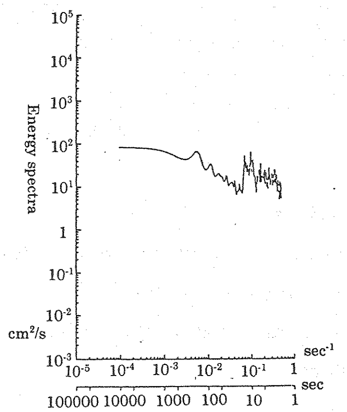

Fig.6 Energy spectra of vertical velocity fluctuation (At D-2)

Table 2 provides the calculated results of the vertical eddy viscosity / diffusivity and the related parameters by each algorithm. The comparison of the vertical eddy viscosity at D-1 and D-2 suggests that the effect of discharge flow at D-2 was stronger than D-1. The value of vertical eddy viscosity at AD-1 was larger than D-1 and D-2. Because AD-1 is located closer to the outlet than D-1 and D-2, this result suggests that the obtained values of vertical eddy viscosity are valid.

The values of vertical eddy diffusivity at D-2 and AD-1 indicated 1～2cm²/s, which are a smaller order of magnitude than the vertical eddy viscosity. This result suggests that the thermal stratification induced by discharge flow held down the thermal diffusion of forced plume more than the momentum diffusion.

Table 2 Vertical eddy viscosity / diffusivity and relative parameters evaluated from observed data

Unit : the cgs system

Measuring site	D-1	D-2	AD-1
Measuring layer	3.0m above the bottom.	3.0m above the bottom.	3.25m above the bottom.
A_{z1}	3.0	6.0	-
A_{z2}	7.5	11.7	23.9
K_{z1}	-	1.2	-
K_{z2}	-	-	1.5
σ_w^2	4.8	8.8	-
$-\overline{u'w'}$	0.69	0.58	1.3
$\partial u / \partial z$	0.092	0.050	0.052
$-\overline{T'w'}$	-	0.0026	-
$\partial T / \partial z$	-	0.0022	-
ε	-	-	0.0091
N	-	-	0.035

NUMERICAL SIMULATION

1. Governing Equations

A 3-dimensional turbulence closure model(k-ε model) was applied to simulate the behavior of the surface forced plume observed in the field. Nakashiki et al.(2) simulated a horizontal buoyant jet discharged from a submerged multi-port diffuser using this model, and the performance was very well. The governing equations in which the Boussinesq approximation is employed are written as follows;

Conservation of mass: $\frac{\partial U}{\partial x}+\frac{\partial V}{\partial y}+\frac{\partial W}{\partial z}=0$ (5)

Conservation of momentum:

$$\frac{\partial U}{\partial t}+U\frac{\partial U}{\partial x}+V\frac{\partial U}{\partial y}+W\frac{\partial U}{\partial z}=-\frac{1}{\rho}\frac{\partial P}{\partial x}+A\left(\frac{\partial^2 U}{\partial x^2}+\frac{\partial^2 U}{\partial y^2}+\frac{\partial^2 U}{\partial z^2}\right) \quad (6)$$

$$\frac{\partial V}{\partial t}+U\frac{\partial V}{\partial x}+V\frac{\partial V}{\partial y}+W\frac{\partial V}{\partial z}=-\frac{1}{\rho}\frac{\partial P}{\partial y}+A\left(\frac{\partial^2 V}{\partial x^2}+\frac{\partial^2 V}{\partial y^2}+\frac{\partial^2 V}{\partial z^2}\right) \quad (7)$$

$$\frac{\partial W}{\partial t}+U\frac{\partial W}{\partial x}+V\frac{\partial W}{\partial y}+W\frac{\partial W}{\partial z}=-\frac{1}{\rho}\frac{\partial P}{\partial y}+A\left(\frac{\partial^2 W}{\partial x^2}+\frac{\partial^2 W}{\partial y^2}+\frac{\partial^2 W}{\partial z^2}\right)+\beta\left(T-T_s\right)g \quad (8)$$

Conservation of temperature: $\frac{\partial T}{\partial t}+U\frac{\partial T}{\partial x}+V\frac{\partial T}{\partial y}+W\frac{\partial T}{\partial z}=K\left(\frac{\partial^2 T}{\partial x^2}+\frac{\partial^2 T}{\partial y^2}+\frac{\partial^2 T}{\partial z^2}\right)$ (9)

Density equation: $\rho=F(T,S)$ (10)

Conservation of k:

$$\frac{\partial k}{\partial t}+\frac{\partial Uk}{\partial x}+\frac{\partial Vk}{\partial y}+\frac{\partial Wk}{\partial z}=\frac{\partial}{\partial x}\left\{(C_k+\nu)\frac{\partial k}{\partial x}\right\}+\frac{\partial}{\partial y}\left\{(C_k+\nu)\frac{\partial k}{\partial y}\right\}+\frac{\partial}{\partial z}\left\{(C_k+\nu)\frac{\partial k}{\partial z}\right\}+P_k+P_b-\varepsilon \quad (11)$$

Conservation of ε :

$$\frac{\partial \varepsilon}{\partial t}+\frac{\partial U\varepsilon}{\partial x}+\frac{\partial V\varepsilon}{\partial y}+\frac{\partial W\varepsilon}{\partial z}=$$

$$\frac{\partial}{\partial x}\left\{(C_\varepsilon+v)\frac{\partial \varepsilon}{\partial x}\right\}+\frac{\partial}{\partial y}\left\{(C_\varepsilon+v)\frac{\partial \varepsilon}{\partial y}\right\}+\frac{\partial}{\partial z}\left\{(C_\varepsilon+v)\frac{\partial \varepsilon}{\partial z}\right\}+\frac{\varepsilon}{k}(C_{\varepsilon 1}P_k-C_{\varepsilon 2}\varepsilon+C_{\varepsilon 3}P_b) \quad (12)$$

Production term:

$$P_k=-\left(\overline{uu}\frac{\partial U}{\partial x}+\overline{uv}\frac{\partial U}{\partial y}+\overline{uw}\frac{\partial U}{\partial z}+\overline{vu}\frac{\partial V}{\partial x}+\overline{vv}\frac{\partial V}{\partial y}+\overline{vw}\frac{\partial V}{\partial z}+\overline{wu}\frac{\partial W}{\partial x}+\overline{wv}\frac{\partial W}{\partial y}+\overline{ww}\frac{\partial W}{\partial z}\right) \quad (13)$$

Buoyancy term: $P_b=\beta g\overline{w\theta}$ (14)

Where U, V, W, u, v, and w are mean and fluctuation velocities in the x, y and z directions, P is dynamic pressure, ρ is density, A and K are eddy viscosity/diffusivity, g is gravitational acceleration, β is coefficient of thermal expansion, T and θ are mean and fluctuation temperature, T_s is ambient temperature, $F(T,S)$ is Kunudsen's formula, k is turbulent energy, ε :dissipation rate, $\overline{uu}, \overline{uv}, \overline{uw}, \overline{vu}, \overline{vv}, \overline{vw}, \overline{wu}, \overline{wv}$ and, $\overline{ww}$ are Reynolds stresses, $\overline{u\theta}$, $\overline{v\theta}$, and $\overline{w\theta}$ are thermal flux, ν is molecular viscosity and

$C_k=0.09$ $C_\mu=0.09$ $P_{rt}=0.7$ $C_\varepsilon=0.07$ $C_{\varepsilon 1}=1.44$ $C_{\varepsilon 2}=1.92$
$C_{\varepsilon 3}=1.4$ $C_\theta=0.13$ $C_{\theta 1}=0.62$.

2. Eddy viscosity / diffusivity

The primary force causing the turbulence in the area near the outlet is discharge flow, and is ambient current and fluctuation in the area far from the outlet. Therefore, the eddy viscosity in the model was defined by following equation;

$$A=\max(A_a, A_t) \quad (15)$$

where A_a is eddy viscosity induced by ambient turbulence, A_t is eddy viscosity induced by discharge flow, and

$A_a=0.01\times L^{4/3}$ (Horizontal) (16)
$A_a=A_0(1+3R_i)^{-1}$ (Vertical) (17)
$A_t=\nu+C_\mu k^2/\varepsilon$ (Horizontal) (18)
$A_t=\nu+C_\mu(1+3R_i)^{-1}k^2/\varepsilon$ (Vertical) (19)

where L is distance from coastal line, $A_0=5\text{cm}^2/\text{s}$, $C_\mu=0.09$, R_i is local Richardson number. Equation (16) is based on the Richardson's 4/3 power law. The maximum A_a of $5\times10^4\text{cm}^2/\text{s}$ in alongshore direction and $1\times10^4\text{cm}^2/\text{s}$ in offshore direction was on the basis of observational data. Equation (17) and (19) employed the stratification function proposed by S. Bloss(4).

As in the case of eddy viscosity, the eddy diffusivity in the model was defined by following equation;

$$K = \max(K_a, K_t) \tag{20}$$

where K_a: eddy diffusivity induced by ambient turbulence, K_t: eddy diffusivity induced by discharge flow, and

$$K_a = 0.01 \times L^{4/3} \quad \text{(Horizontal)} \tag{21}$$
$$K_a = K_0 (1+3R_i)^{-3} \quad \text{(Vertical)} \tag{22}$$
$$K_t = k_T + C_\mu k^2 / P_r \varepsilon \quad \text{(Horizontal)} \tag{23}$$
$$K_t = k_T + C_\mu (1+3R_i)^{-3} k^2 / P_r \varepsilon \quad \text{(Vertical)} \tag{24}$$

where K_0=5cm²/s, k_T: molecular thermal diffusivity, P_r: turbulent Prandtl number (=0.7).

3. Computational Method

Computation was carried out using the following computational methods;

1) The hydraulic pressure was calculated using HSMAC method.
2) FAVOR (Fractional Area/Volume Obstacle Representation) method(5) was employed in order to represent the topography of sea bottom accurately.
3) TVD(Total Variation Diminishing) scheme(6) was employed for advection term of the scalar quantities T, k and ε to avoid the numerical diffusion due to the coarse mesh near the outlet.

4. Computational Conditions

The computational domain is about 8.7km in the north-south direction, and about 6km in the east-west direction. The origin was set at the outlet. The sizes of computational grid were varied in the range from 2.12m to about 1000m horizontally, and from 0.5m to 5.6m vertically. The numbers of the grids in the whole domain were 71 in a north-south direction, 42 in the east-west direction and 25 in the vertical direction.

The boundary conditions used are shown in Table 3. The discharge conditions were described in the earlier chapter "FIELD OBSERVATION". The numbers of the grids in the outlet was 3 in the horizontal direction and 5 in the vertical direction. The boundary conditions of k and ε at the outlet were as follows;

$$k = \alpha U^2 \tag{25}$$
$$\varepsilon = C_\mu k^{3/2} / H_0 \tag{26}$$

where α=0.002, U is discharge velocity, C_μ=0.09, H_0 is height of the outlet.

The condition of ambient current was set to 20cm/s at the 2km offshore point.

Table 3 Boundary Conditions

	Shore line Bottom	Outflow B.C.	Inflow B.C.	Surface
Velocity	FreeSlip	$\frac{\partial u,v}{\partial n}=0$	Constant	Free surface
Dynamic pressure	$\frac{\partial P}{\partial n}=0$	0	$\frac{\partial P}{\partial n}=0$	$\frac{\partial P}{\partial n}=0$
Temperature	$\frac{\partial T}{\partial n}=0$	$\frac{\partial T}{\partial n}=0$	Ambient temperature (15.2℃)	Heat radiation condition
k	$\frac{\partial k}{\partial n}=0$	$\frac{\partial k}{\partial n}=0$	Constant*	$\frac{\partial k}{\partial n}=0$
ε	$\frac{\partial \varepsilon}{\partial n}=0$	$\frac{\partial \varepsilon}{\partial n}=0$	Constant**	$\frac{\partial \varepsilon}{\partial n}=0$

* $k=\alpha U^2$ ($\alpha=0.002$, U : velocity in normal direction)

** $\varepsilon=C_\mu k^{3/2}/h$ ($C_\mu=0.09$, h: depth)

5. Computational results

Fig.7 (1) shows the computed result of surface distributions of velocity vectors and temperature contours in the whole area 12 hours after the discharge was initiated. The computed distributions agree with the observation results shown in Fig.1 or Fig.2 (1) qualitatively.

A magnified view of Fig.7 (1) in the area near the outlet is shown in Fig.7 (2). This figure indicates the entrainment from both the off-shore side and the near-shore side, and that the forced plume gradually turns to the direction along the shore line.

Fig.8 shows the result of computation attempted to reproduce the vertical structure of velocity and temperature given in Fig.3. The computational results are in good agreement with the observational results.

Fig.9 shows the comparison between the computational and observational results for vertical distribution of the vertical eddy viscosity and diffusivity at AD-1. The observational results suggest that the values of the vertical eddy viscosity and diffusivity in the layers of 2~3m under the surface are relatively large. The characteristics of the calculated distributions and the order of magnitude agree with the observational results. The agreement indicates that the effect of stratification in Equations (17), (19), (22) and (24) is appropriate, and indicates that the model predicts the characteristics of vertical turbulence in jet zone accurately.

On the other hand, the area where the horizontal eddy viscosity and diffusivity were evaluated by Equation (18), (23) was about 30m in alongshore direction and about 30m in offshore direction from the outlet. The maximum values of eddy viscosity and diffusivity in the area were 0.26×10^4cm^2/s and 0.37×10^4cm^2/s respectively.

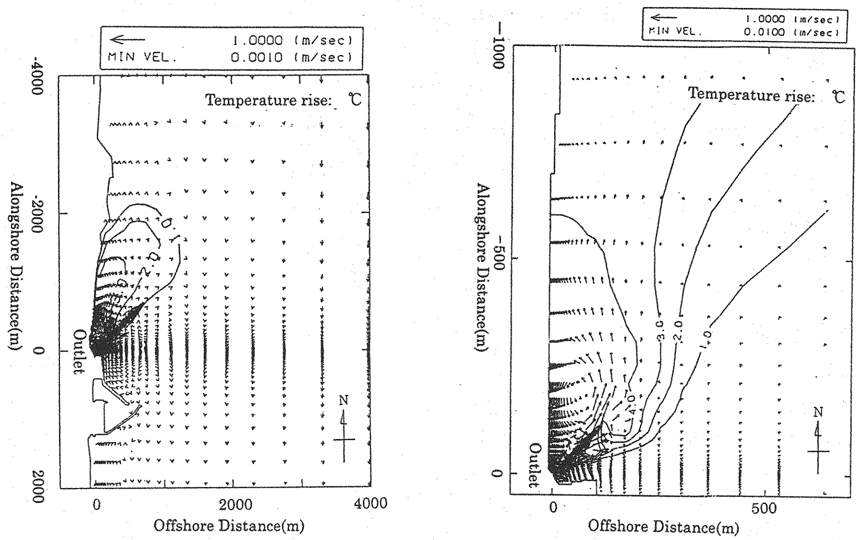

(1) The whole area (2) The area near the outlet

Fig.7 Velocity vectors and temperature contours in the surface (Computational results)

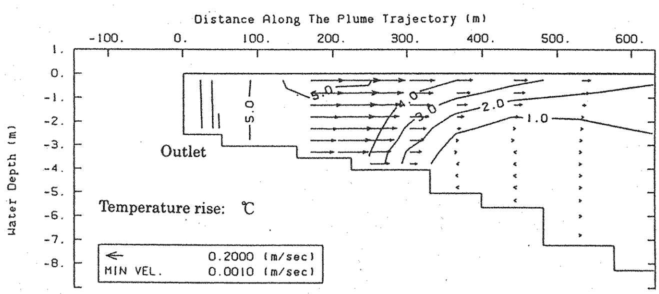

Fig.8 Velocity vectors and temperature contours in vertical section (Computational Result)

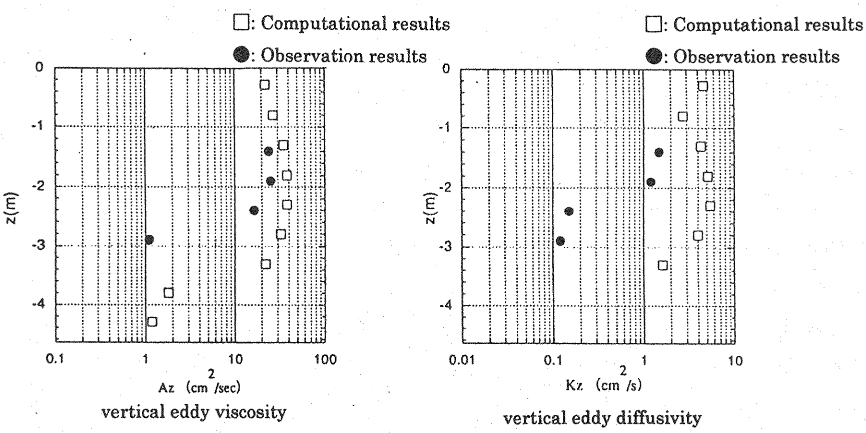

Fig.9 Vertical distributions of vertical eddy viscosity / diffusivity (At AD-1)

CONCLUSION

The 3-dimensional structure and turbulent characteristics of a surface forced plume formed by the discharge of heated water from thermal plant into the sea were investigated by field observation. The 3-dimensional numerical model was applied to simulate the behavior of the surface forced plume observed in the filed. The obtained results were summarized as follows.

1) On the basis of observed distributions of velocity and temperature, the 3-dimensional structure of the current and stratification of the surface forced plume was understood. The trajectory of the forced plume varied by the effects of ambient currents and bottom topography.

2) The vertical eddy viscosity / diffusivity in the area near the outlet were evaluated based on the observed data of velocity and temperature fluctuations. As a result, it was found that the obtained values of vertical eddy viscosity and diffusivity are reasonable. The values of vertical eddy diffusivity proved to be one order smaller than the vertical eddy viscosity.

3) The characteristics of the calculated velocity and temperature distributions agreed with the observational results well.

4) The characteristics of the calculated vertical eddy viscosity / diffusivity and the order of magnitude were consistent with the observation results. The agreement implies that the stratification function employed in this study is available.

5) The 3-dimentional numerical model used in this study indicated a good performance to simulate a surface forced plume observed in the field.

ACKNOWLEDGMENTS

This study was carried out under the grant by the Resource and Energy Agency(MITI/REA) in Japan. The authors were grateful for the members of the committee in this project, giving them many useful suggestions.

REFERENCE

1. Nakashiki, N. , S. Matsunashi, S. Sakai, and K. Maruyama: Diffusion behavior of a Forced Plume Discharged in the Horizontal Direction, Annual Jour. of Hydraulic Engine., JSCE, vol. 40, pp.537-542, 1996(in Japanese).
2. Nakashiki, N. , S. Matsunashi, S. Sakai, T. Tsubono and K. Maruyama: Behavior of a Horizontal Buoyant Jet Discharged from Multiple Pipe, Proceedings of the 6th International Symposium on Flow Modeling and Turbulence Measurements, IAHR, pp.263-270, 1996
3. Sakai, S. , N. Nakashiki, S. Matsunashi, T. Tsubono and K. Maruyama: Calculation of a Forced Plume in a Coastal Area by a Three-Dimentional k-ε model, Proceedings of Measurements and Modeling in Environmental Pollution in Spain, 1997
4. Bloss, S., R. Lehfeldt and J. C. Patterson: Modeling turbulent transport in stratified estuary, J.

Hydr. Eng., Vol. 114, No. 9, pp.1115-1133, ASCE, 1988
5. Hirt, C. J.: A porosity technique for the definition obstacles in rectangular cell meshes, Fourth International Conference on Numerical Ship Hydrodynamics, pp.450-468, 1985.
6. Fujii, K: Numerical Computational Method of Hydrodynamics, Tokyo University Press, pp.51-76, 1994(in Japanese).

APPENDIX – NOTATION

The following symbols are used in this paper:

A = eddy viscosity;
A_a = eddy viscosity induced by ambient turbulence;
A_t = eddy viscosity induced by discharge flow;
$F(T,S)$ = Kunudsen's formula;
g = gravitational acceleration;
h = height of outlet;
K = eddy diffusivity;
K_a = eddy diffusivity induced by ambient turbulence;
K_t = eddy diffusivity induced by discharge flow;
k_T = molecular thermal diffusivity;
k = turbulent energy;
L = distance from coastal line;
N = Brunt-Vaisala frequency;
P = dynamic pressure;
P_r = turbulent Prandtl number;
R_i = local Richardson number;
T = mean temperature;
T_s = ambient temperature
U, V, W = mean velocities in the x, y and z directions;
u, v, w = fluctuation velocities in the x, y and z directions;
$\overline{uu}, \overline{uv}, \overline{uw}, \overline{vu}, \overline{vv}, \overline{vw}, \overline{wu}, \overline{wv}, \overline{ww}$ = Reynolds stresses;
$\overline{u\theta}, \overline{v\theta}, \overline{w\theta}$ = thermal flux;
U = discharge velocity;
β = coefficient of thermal expansion;
$\gamma_w(\tau)$ = auto-correlation coefficient of vertical velocity;
ε = dissipation rate;
θ = fluctuation temperature;,
ν = molecular viscosity;
ρ = density.

(Received November 15, 1999 ; revised March 29, 2000)